Plasma Sources Science and Technology

Carbon nanotube growth by PECVD: a review

To cite this article: M Meyyappan *et al* 2003 *Plasma Sources Sci. Technol.* **12** 205

INSTITUTE OF PHYSICS PUBLISHING PLASMA SOURCES SCIENCE AND TECHNOLOGY

Plasma Sources Sci. Technol. **12** (2003) 205–216 PII: S0963-0252(03)60688-2

Carbon nanotube growth by PECVD: a review

M Meyyappan, Lance Delzeit, Alan Cassell[1] and David Hash

NASA Ames Research Center, Moffett Field, CA 94035, USA

E-mail: meyya@orbit.arc.nasa.gov

Received 18 November 2002, in final form 7 March 2003
Published 2 April 2003
Online at stacks.iop.org/PSST/12/205

Abstract
Carbon nanotubes (CNTs), due to their unique electronic and extraordinary mechanical properties, have been receiving much attention for a wide variety of applications. Recently, plasma enhanced chemical vapour deposition (PECVD) has emerged as a key growth technique to produce vertically-aligned nanotubes. This paper reviews various plasma sources currently used in CNT growth, catalyst preparation and growth results. Since the technology is in its early stages, there is a general lack of understanding of growth mechanisms, the role of the plasma itself, and the identity of key species responsible for growth. This review is aimed at the low temperature plasma research community that has successfully addressed such issues, through plasma and surface diagnostics and modelling, in semiconductor processing and diamond thin film growth.

1. Introduction

The interest in carbon nanotubes (CNTs) and the breadth of research activities across the world on their application potential have been extraordinary in the last decade. CNTs were first discovered by Sumio Iijima of the NEC Corporation in 1991 [1] in the soot of an arc discharge apparatus. These are elongated fullerenes with diameters as small as 0.7 nm and lengths of up to several microns. The interesting combination of electronic and mechanical properties of CNTs [2–4] has led to wide-ranging investigations of their potential in future electronics and computing, field emitter devices, sensors, electrodes, high strength composites, and storage of hydrogen, lithium and other metals. The early processes used for CNT production were laser ablation and an arc discharge approach. Both are able to produce single-walled and multiwalled carbon nanotubes (SWCNTs, MWCNTs) and continue to be used by researchers. Details on these two processes can be found in [1, 4–6]. Of the two, laser ablation is not amenable for scaleup whereas the arc discharge process has been used to produce large quantities of CNTs. The purity of the latter process is rather modest with the majority of the impurity being amorphous carbon. The laser ablation technique has been able to produce SWCNTs with a purity as high as 90%.

Chemical vapour deposition (CVD) has been widely used to grow CNTs in recent years. In this approach, a feedstock such as CO or a hydrocarbon is heated to 800–1000°C with a transition metal catalyst to promote nanotube growth [7–14]. It has been shown [9, 10, 14] that CVD is amenable for nanotube growth on patterned surfaces, suitable for fabrication of electronic devices, sensors, field emitters and other applications where controlled growth over masked areas is needed for further processing. More recently, plasma enhanced CVD (PECVD) has been investigated for its ability to produce vertically-aligned nanotubes. A variety of plasma sources and widely varying results have been reported in the literature [15–42]. Diagnostics and modelling of the PECVD reactor, however, have not received any attention except a simple emission analysis [37] and a zero-dimensional model [43] of the plasma.

The purpose of this paper is to review the current status of CNT growth by PECVD and point out areas where further work is warranted. This paper is organized as follows. A brief discussion of CNT properties is given in section 2. Section 3 provides an overview of the PECVD growth apparatus and precursor sources used in nanotube growth. Catalyst preparation techniques are outlined in section 4. Some examples of growth results reported in the literature are presented in section 5. Growth mechanism is the subject of section 6. A brief discussion on the applications of the CNTs is given in section 7. Finally, a summary of challenges and directions for future work are presented in the concluding remarks.

[1] Also at: Eloret Corporation.

2. Properties of CNTs

A SWCNT is a rolled-up tubular shell of graphene sheet which is made up of benzene-type hexagonal rings of carbon atoms (figure 1). The structure is conveniently expressed in terms of a one-dimensional unit cell, as shown in figure 1. The circumference of a SWCNT is given by the chircal vector $\boldsymbol{C} = n\boldsymbol{a} + m\boldsymbol{b}$ where n and m are integers and $\boldsymbol{a}$ and $\boldsymbol{b}$ are unit vectors of the hexagonal lattice. The diameter of the nanotube is given by $\sqrt{3}a_{\text{c–c}}(m^2 + mn + n^2)^{0.5}$ where $a_{\text{c–c}}$ is the C–C bond length. SWCNTs exhibit unique electronic properties in that they can be metallic or semiconducting depending on their chirality. This allows formation of semiconductor–semiconductor, and semiconductor–metal junctions useful in device fabrication. SWCNTs also possess extraordinary mechanical properties. The Young's modulus of individual SWCNTs has been estimated to be around 1 TPa and the yield strength can be as large as 120 GPa [2].

A MWCNT is a stack of graphene sheets rolled up into concentric cylinders (see figure 2). The walls of each layer of the MWCNT, i.e. the graphite basal planes, are parallel to the central axis ($\theta = 0$). In contrast, a stacked-cone arrangement (also known as Chevron, bamboo, ice cream cone, or piled cone structures) is also seen where the angle between the graphite basal planes and the tube axis is nonzero [44]. Nolan *et al* [44] suggest that hydrogen, added during the growth process, satisfies the valences at cone edges in such structures. A MWCNT, in contrast, has no graphite edges and therefore there is no need for valence-satisfying species such as hydrogen. Since the stacked-cone structures exhibit only small θ values and are not solid cylinders but are mostly hollow, they can be called multiwalled carbon nanofibres (MWCNFs) [37]. Note that the terminologies graphitic carbon fibres (GCFs) and vapour-grown carbon fibres (VGCFs) have long been used to denote solid cylinders. Early developments of carbon filaments (solid cylindrical structures) have been discussed in [45–48].

3. Nanotube growth: reactor and procedures

As markets for CNTs are not yet developed and the current research is primarily academic, there is no commercial equipment industry now, unlike the case with integrated circuit (IC) manufacturing; so the growth hardware is mostly home-made. The plasma enhancement in CVD first emerged in microelectronics because certain processes cannot tolerate the high wafer temperatures of the thermal CVD. For example, charring of photoresists on patterned wafers is a problem at elevated temperatures of the thermal CVD operation. The plasma CVD allows an alternative at substantially lower wafer temperatures (room temperature to 100°C) for many processes and hence has become a key step in IC manufacturing. The low temperature operation is possible because the precursor dissociation (necessary for the deposition of all common semiconductor, metal and insulator films) is enabled by the high energy electrons in an otherwise cold plasma.

In contrast to the above familiar scenario, CNT growth does not need precursor dissociation in the gas phase. This is evident from thermal CVD of nanotubes, where the growth temperature is maintained below the pyrolysis temperature of the precursor hydrocarbon gas to minimize gas phase dissociation. The precursor dissociation occurs at

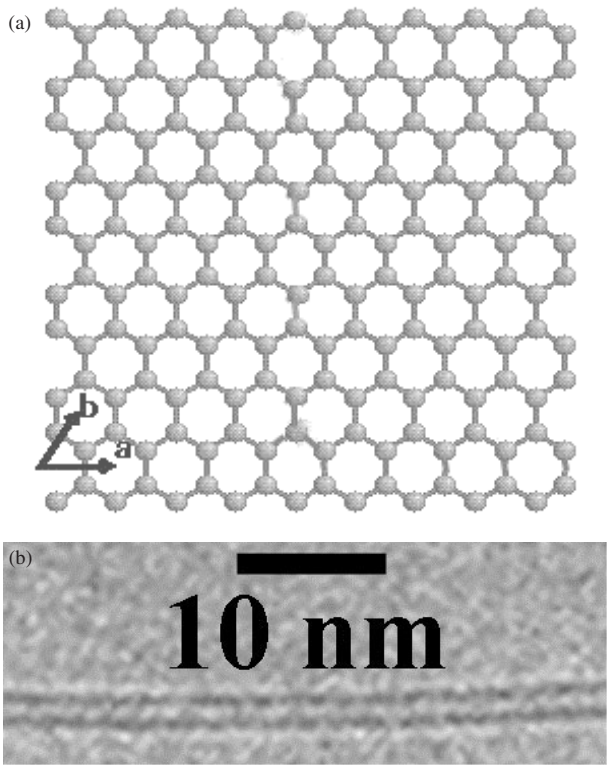

Figure 1. (*a*) Two-dimensional graphene sheet showing the chiral vector. (*b*) TEM image of a SWCNT.

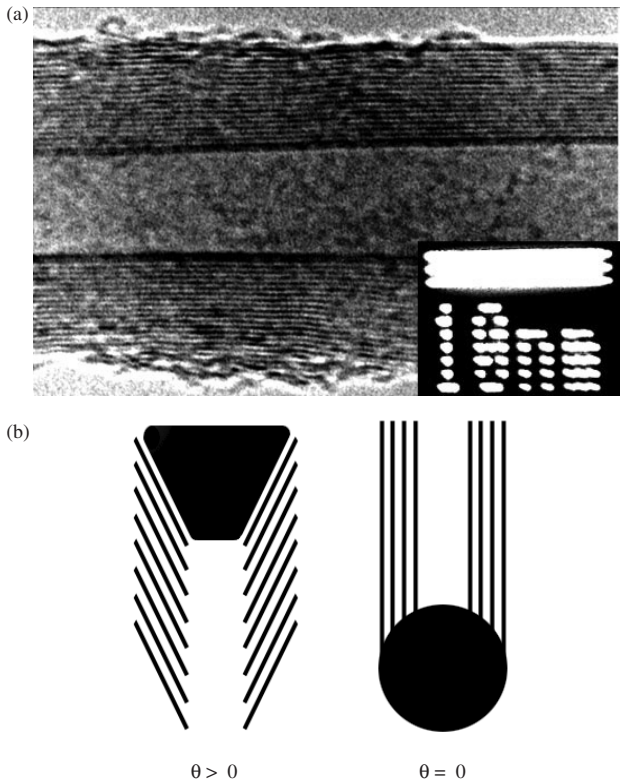

Figure 2. (*a*) TEM image of a MWCNT. (*b*) Structure of a MWCNT ($\theta = 0$) and MWCNF ($\theta > 0$).

the surface of catalyst particles producing the carbon needed for nanotube growth, as will be seen in section 6. Franklin and Dai [49] analysed the gas phase in a CVD reactor with methane feedstock using mass spectroscopy and found very little of other components, besides CH_4, at 900°C. This is also consistent with the findings from a two-dimensional flow and chemical model of the same reactor [43]. Given this scenario, the well-known efficiency of a plasma to tear apart the precursor gas for reactive radical generation should not be a factor. What is known to date about the catalytic activity of the transition metal particles for CNT growth tells us that growth does not occur below 550°C. Hence, the cold wafer scenario is out of the question, at least for now, until new knowledge emerges. It is not clear then what the true role of the plasma in CNT growth is, despite a large number of articles in this field [15–42]. However, there is enough empirical evidence that the electric field in the plasma enables more vertically aligned CNTs than thermal CVD [24, 27, 32, 37]. Whereas any marginal alignment seen in thermal CVD samples is due to a crowding effect (nanotubes supporting each other by van der Waals attraction), individual, free-standing and vertically-oriented CNTs are possible with PECVD, as will be seen in section 5. This in itself is an adequate reason to pursue PECVD for growing CNTs. All other possible reasons such as lower substrate temperature, more knobs to control the process, morphology etc are not clear at present.

As in the case of earlier technology waves such as microelectronics materials and diamond deposition, researchers have attempted a variety of plasma sources for CNT growth: dc [27–30, 32–35, 42], hot-filament aided with dc [15, 16, 18, 41], rf [31], microwave [17, 19–26, 36, 40], inductively coupled plasma reactors [37–39] and rf with magnetic enhancement [50, 51].

For an overview of the fundamentals of cold plasma in materials processing and plasma reactors, the reader is referred to [52]; here a brief discussion of the various reactors reported in the literature is presented. A dc plasma reactor consists of a pair of electrodes in a grounded chamber with one electrode grounded and the second connected to a power supply. The negative dc bias applied to the cathode leads to a breakdown of the feedgas. The wafer with the catalyst layer may be placed either on the anode or cathode for CNT deposition. The electrode holding the wafer may need an independent heating source to raise the wafer temperature to the desired growth temperature. Instead of a resistive heater underneath the electrode, a tungsten wire suspended in the plasma stream may serve as the heating source. This is the so-called hot-filament system with plasma assistance. These two systems have successfully yielded MWCNTs and MWCNFs as evidenced from [15, 16, 18, 27–30, 32–35, 41, 42]. However, the negative bias on the wafer in these systems appears to be very high (>300 V). It is well known that ions gain substantial energy in the sheath from high electric fields, and the high energy ion bombardment of the wafer often leads to damage which is well known from silicon and III–V semiconductors literature. Because of this, and the poor efficiency of the dc systems, the semiconductor industry abandoned these sources a couple of decades ago.

Typical hydrocarbon sources used in plasma-based growth of CNTs include methane, ethylene and acetylene. Since the plasma can dissociate the hydrocarbon creating a lot of reactive radicals, the use of pure hydrocarbon feedstock may lead to substantial amorphous carbon deposition. Therefore, it is desirable to dilute the hydrocarbon with argon [37], hydrogen [21, 37] or ammonia [18, 24, 27]. The pressure in the reactor typically ranges from 1 to 20 Torr with a hydrocarbon fraction of up to 20%. Note that this is much higher than what is common in diamond deposition where the hydrocarbon fraction is typically around 1%. Atmospheric pressure operation of plasma systems is uncommon due to power coupling problems. Low pressure operation in the tens of milliTorr would result in very slow growth rates. So, PECVD reactors are typically operated at 1–20 Torr pressure levels for CNT growth. At these pressure levels, inductive coupling to hydrocarbon/H_2 systems appears to be difficult; the coupling appears to have a large capacitive component [37–39]. The capacitive component decreases with an increasing fraction of argon. The E–H mode transition in inductive reactors is a function of the gas, nature of diluent, pressure and power [53]. Microwave sources are very popular at these pressures and power levels of up to 2 KW and have been widely used for diamond deposition. Following this success, CNT literature also consists of several successful demonstrations of MWCNT growth using microwave sources [17, 19–26, 36, 40]. In the case of high density plasma sources, the substrate-holder may be biased with a dc or rf power supply to independently control the bias on the wafer. More recently, rf sources with magnetic enhancement have also been reported [50, 51].

In addition to the plasma source, matching network and other power coupling components, the equipment consists of mass flow controllers and one or more vacuum pumps (see figure 3). The growth chamber itself is grounded. All plasma reactors are cold-wall systems with the substrate directly heated using some form of heat source from below the substrate-holder. First, the wafer with the catalyst is loaded in the reactor and the system is pumped down to 10^{-5} Torr or below to minimize impurities and water vapour. The substrate-holder is heated to the desired temperature. Then the feedstock is admitted, and the flow rate and chamber pressure can be set to desired levels independent of each other with the aid of a throttle valve. Next, the power from the power source is coupled to the plasma. At the end of the run, the heater, power source and the gas flow are turned off and the system is purged with argon flow to cool the reactor. The wafer is removed after the reactor cools down below 300°C. Exposure to air at high temperature will damage the nanotubes.

4. Catalyst preparation

Transition metal catalysts are needed for CNT growth by PECVD. Note that amorphous carbon or diamond (depending on plasma and surface conditions) will result in the absence of such catalysts. It is believed that the catalyst on the substrate must be in the form of particles instead of smooth, continuous films. There have been several studies indeed correlating the catalyst particle size and the diameter of the resulting nanotubes [22, 28, 31, 33]. The metals used to date as catalysts include Fe, Ni, Co, and Mo. It is possible to apply these onto the substrate from solutions containing them or they can be directly deposited using some physical techniques. These two

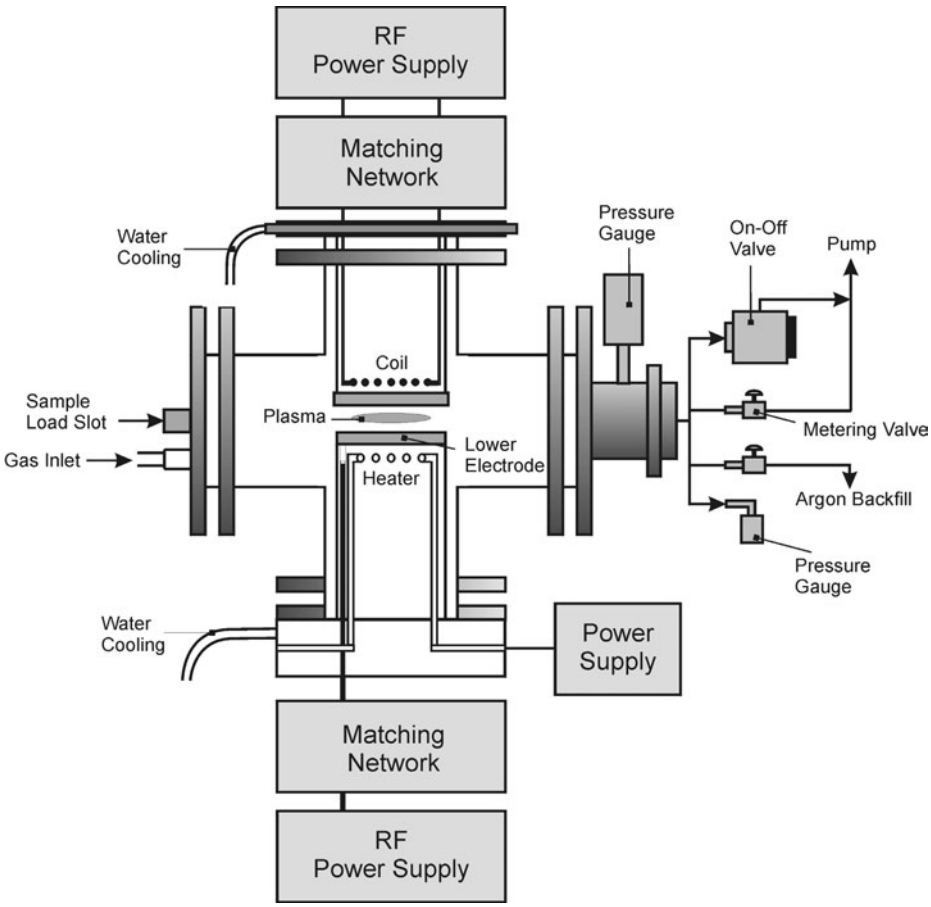

Figure 3. Schematic of a PECVD set-up.

approaches are different in terms of required resources, time and cost, and the nature of the resulting products.

The literature contains numerous recipes for preparing catalysts from solutions and one such recipe is given below [12]. First, 0.5 g (0.09 mmol) of Pluronic P-123 triblock copolymer is dissolved in 15 cc of a 2 : 1 mixture of ethanol and methanol. Next, $SiCl_4$ (0.85 cc, 7.5 mmol) is slowly added using a syringe into the triblock copolymer/alcohol solution and stirred for 30 min at room temperature. Stock solutions of $AlCl_3 \cdot 6H_2O$, $CoCl_2 \cdot 6H_2O$, and Fe $(NO_3)_3 \cdot 6H_2O$ are prepared at the concentration of the structure directing agent (SDA) and inorganic salts. The catalyst solutions are filtered through 0.45 μm polytetrafluoroethylene membranes before applying onto the substrate. The substrate with the catalyst formulation is loaded into a furnace and heated at 700°C for 4 h in air to render the catalyst active by the decomposition of the inorganic salts and removal of the SDA. This completes the catalyst preparation and the substrate is ready for loading into the growth chamber.

Solution-based preparation techniques are more common in thermal CVD. A typical preparation includes such steps as dissolution, stirring, precipitation, refluxing, separation, cooling, gel formation, reduction, drying/annealing/calcination etc. The overall process is cumbersome and time consuming; some recipes even call for overnight annealing. Another problem is the difficulty in confining the catalyst within small patterns. Physical techniques such as electron gun evaporation [27–30], thermal evaporation [33], ion beam sputtering [10, 11, 37–39] and magnetron sputtering [18, 21, 22, 31, 42] have also been successfully used in catalyst preparation. These techniques are quick, easy, and amenable to produce small patterns, in contrast to the solution-based approaches. Typically, a thin catalyst film (<20 nm) is applied by these techniques. The eventual particle size and the resultant nanotube diameter seem to correlate to film thickness. Thinner films in general lead to smaller particles and tube diameters [28, 33]. While a small grain size is not guaranteed in as-prepared films, further insurance steps are taken to break the film into desired particles. For example, in PECVD techniques, an inert gas plasma or hydrogen plasma is run first prior to admitting the feedgas and initiating growth [19, 23], where the plasma ion bombardment helps to create particles. In some cases, particularly with Ni films, a pretreatment with NH_3 has been used where Ni is etched into small particles [18, 27, 42]. Delzeit *et al* [10, 11, 37, 38] have shown that introduction of a metal underlayer (such as Al) can be used instead of any chemical pretreatment steps. Thermodynamics and kinetic studies [44] indicate that alloying a catalyst with a noncatalystic metal increases the number of reactive sites through surface clusters. In addition, an underlayer such as Al allows tuning of the final conductivity of the substrate with the CNTs. The metal underlayer may also play the role of a barrier layer between an incompatible substrate and catalyst metal to prevent back-diffusion which, for example, is the case with Fe and a highly oriented pyrolytic graphite substrate.

5. Growth results

Bower *et al* [24] showed the effect of electric field on alignment of nanotubes unambiguously in a microwave plasma of acetylene and ammonia. Initially when the plasma was on, their MWCNTs were vertical; when growth was continued with plasma off (in a thermal CVD mode), the nanotubes were found to be curly or randomly oriented. They also found that nanotubes always grew perpendicular to the substrate surface regardless of the substrate position or orientation. Since their work, a number of articles have appeared where the general orientation of PECVD-grown nanotubes, as seen in scanning electron microscopic (SEM) images, is better than the results from thermal CVD.

Figure 4 shows MWCNFs grown in a dc plasma assisted hot-filament CVD (dc-HFCVD) reactor with an acetylene + ammonia feedstock diluted with argon. Here, the MWCNFs are individual, free-standing and well-aligned. This growth follows tip growth mechanism as evidenced by particles at the top end. Figure 5 shows MWCNTs grown in an ICP reactor with an ethylene + H_2 feedstock. The coil power is 100 W and the rf capacitive power at the bottom electrode is 200 W. The catalyst here consists of a 10 nm layer of Fe with underlayers of 20 nm Ti and 10 nm Al to improve the substrate conductivity. A 10 min growth at 3.5 Torr and 900°C yields nearly a 10 μm tall tower of MWCNTs. In this case, the catalyst particles stay at the bottom, representing the base growth case. Base versus tip growth mechanism will be discussed further in section 6.

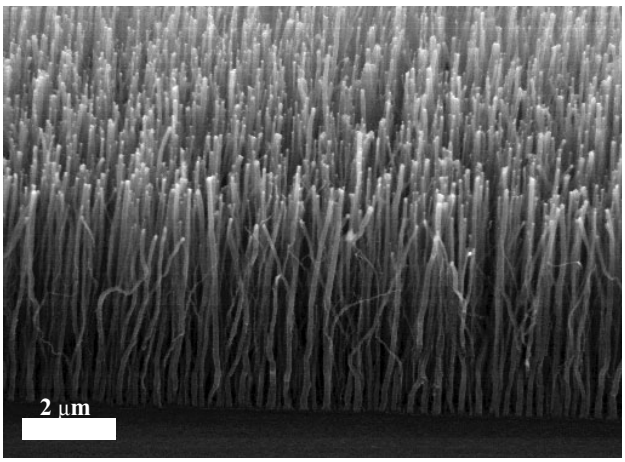

Figure 4. High magnification SEM images of MWCNF grown a dc-HFCVD reactor at a bias of −550 V (360 W, 670 mA) from photolithographically patterned nickel catalyst sites. Growth time: 20 min.

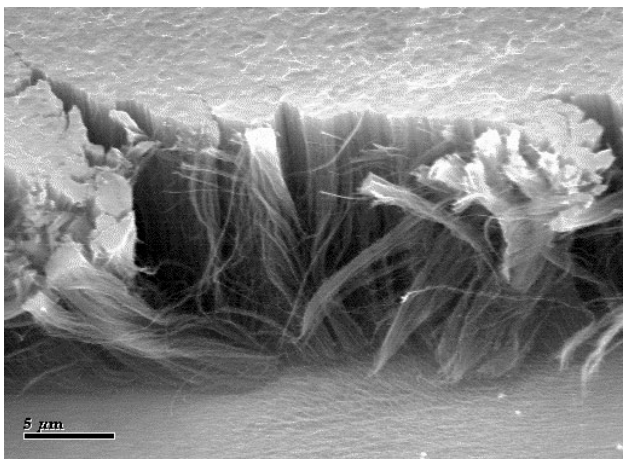

Figure 5. MWCNT grown in an inductive plasma reactor. Conditions: 900°C; 3.5 Torr; 20 sccm C_2H_4/80 sccm H_2; 100 W inductive power; 200 W capacitive power; −280 V substrate bias; catalyst: 20 nm Ti/10 nm Al/10 nm Fe; 10 min growth.

Figure 6 shows a TEM image of a MWCNF with a particle at the tip. The disordered structure in the core, as shown in figure 2(*b*), is evident. Delzeit *et al* [37] first showed that an increase in capacitive bias on the substrate can transition from MWCNTs (as in figure 5) to MWCNFs (as in figure 4). Similarly, an increase in argon dilution was also shown to transition from MWCNFs to MWCNTs. They speculated, in both cases, that a change in atomic hydrogen environment near the wafer (whether it is due to local dc bias or argon dilution), may be responsible for the observed transition. Some preliminary evidence of atomic H intensity from optical emission spectroscopy was used to arrive at this speculation. In this system, though the temperature of the substrate-holder block is kept constant at a desirable setting, the wafer temperature itself was not monitored; but the observed structural transitions are not expected to be the result of temperature changes. Though the above results in [37] are from an ICP reactor with an rf power supply at the bottom electrode, structural transition with substrate bias happens in dc-HFCVD as well (see figure 7). Figure 7(*a*) shows MWCNFs under a dc power of 360 W and bias of −550 V. When these are raised to 400 W and −575 V, a mixture of MWCNTs and MWCNTs is the result. When the power and dc bias reach 470 W and −600 V, only MWCNTs are seen. Note here that the feedstock is acetylene + ammonia which is different from the methane + H_2 in [37]. The bias effect in dc-HFCVD seems to be the opposite of that in [37] for the ICP reactor. It is important to recognize that in dc-HFCVD, the wafer temperature is not kept constant. As the wafer bias and power to the substrate increases, the wafer temperature is

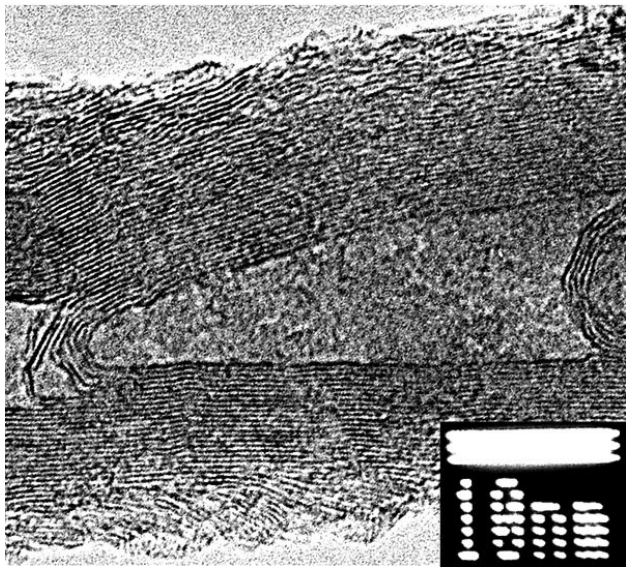

Figure 6. TEM image of a MWCNF.

expected to increase which can result in the rearrangement of catalyst particles into large clusters. Such a change can affect the final morphology of the nanotubes. Careful studies and diagnostics are needed to isolate the effects of substrate bias as well as other parameters.

Comparison of the PECVD results in the literature indicates growth rates (at the initial stage) of 0.5–6 μm min^{-1}, with a level-off after 20 min or so. In all cases, growth stoppage is possible due to the covering of the particles with an amorphous carbon overcoat, i.e. catalyst poisoning. This in itself should not be a surprise, given the abundance of active radicals in the plasma system (discussed in section 6). The growth rate in PECVD generally appears to be smaller than that in thermal CVD, which may be partly due to the atmospheric pressure operation of thermal CVD.

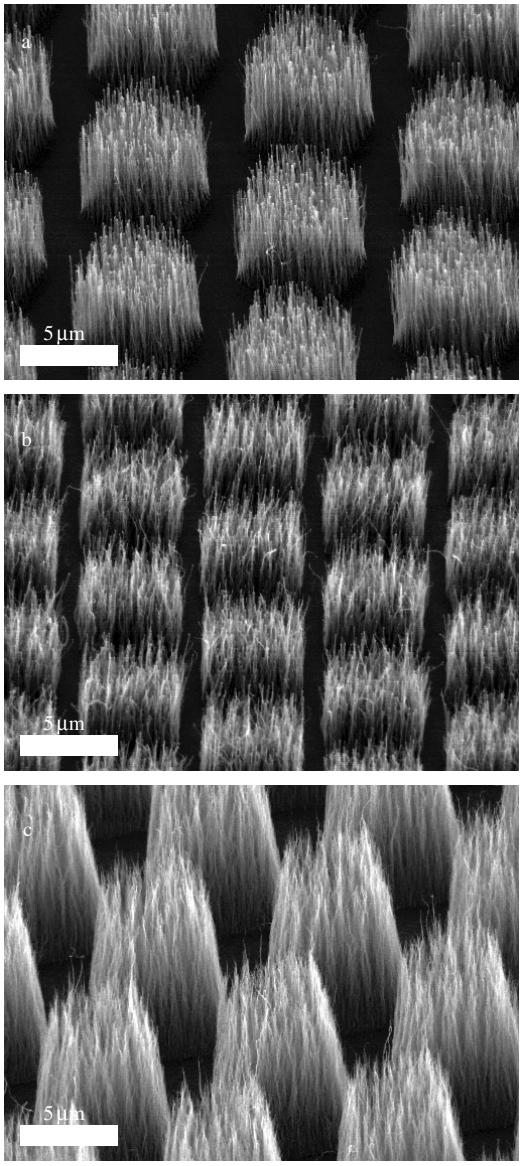

Figure 7. Increasing the bias changes the CNT growth morphology. The CNTs were grown from patterned 20 nm thick nickel catalyst film on a 100 nm thick chromium underlayer, all patterned using photolithography. Process gas mixture consisted of 80 sccm NH_3 and 30 sccm C_2H_2 at 4 Torr. Panel A shows the exclusive growth of well-aligned MWCNFs at a bias voltage of −550 V (360 W, 670 mA). Panel B, grown at −575 V bias (400 W, 710 mA) shows a mixture of MWCNFs and MWCNTs. Panel C, further increasing the bias to −600 V (470 W, 780 mA) gives exclusive growth of MWCNTs (note the absence of catalyst particles at the tips of the CNTs).

Figure 8 shows the effect of growth temperature on MWCNT production in an ethylene + H_2 system. The reactor conditions are 3 Torr, 100 W inductive power and 200 W rf power at the substrate, and a 10 nm Fe catalyst on a silicon substrate. Below 600°C, there is not much growth and serious growth happens at and above 700°C here. Though it is not obvious from the SEM images of figure 8, a careful analysis (through counting from TEM images) indicates that the average diameter of MWCNFs increases with temperature. Though the starting catalyst is 10 nm iron in all cases, an increase in temperature may rearrange the particles into different size clusters. The average height of the MWCNFs decreases with an increase in temperature. Combining the results for the height and diameter, one can conclude that

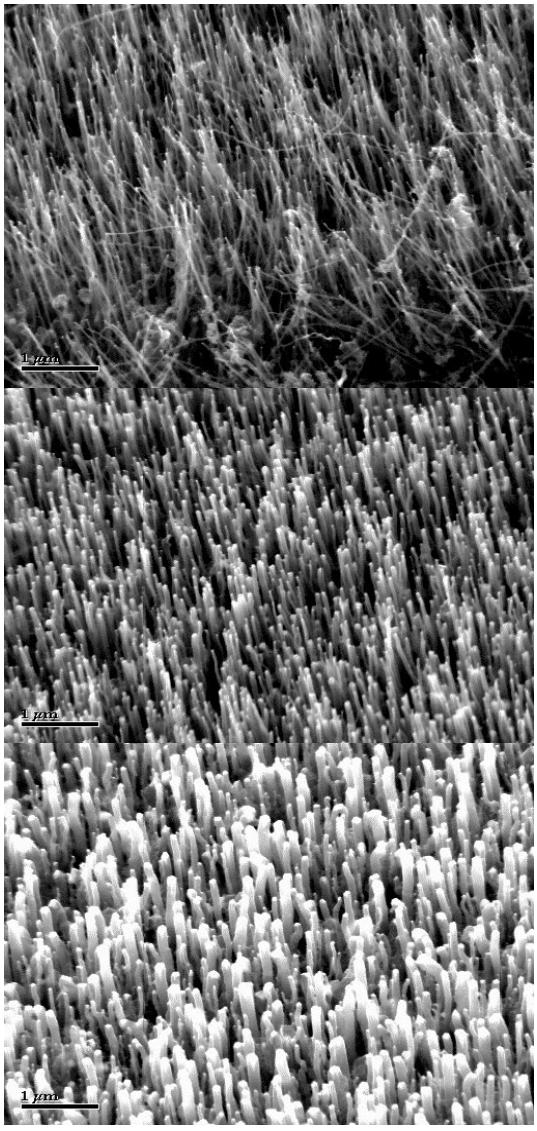

Figure 8. Effect of temperature on growth characteristics for MWCNFs grown in an ICP reactor at 3 Torr, 20/80: C_2H_4/H_2 for a total flow of 100 sccm, 100 W inductive power, 200 W capacitive power and a 10 nm thick iron catalyst.

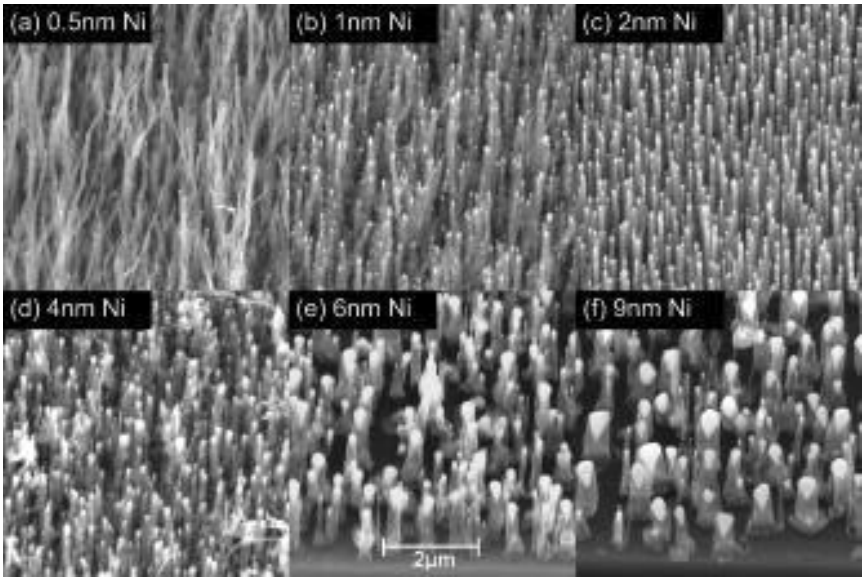

Figure 9. Effect of catalyst layer thickness. DC plasma of C_2H_2/NH_3. Reproduced with permission from [33].

thicker fibres grow slower. The same conclusion has been reached for other reactors and feedstock systems as discussed in [25, 33]. Indeed, for carbon diffusion-controlled situations, Baker *et al* [46] present a simple analysis showing that the carbon flux escaping the growth-side of the particle and hence the growth rate vary inversely with the radius of the particle.

The particle radius is also a function of the initial catalyst layer thickness in addition to the prevailing substrate temperature, ion energy and other factors. Under otherwise identical temperature, substrate bias etc, thicker catalysts lead to shorter and fatter MWCNFs, as evident from figure 9. This investigation uses a catalyst (Ni) as thin as 0.5 nm and obtains good growth; but the absence of catalyst does not yield any nanotubes.

Investigations of hydrocarbon fraction in the mixture indicate that at low concentrations of hydrocarbon when the total carbon supply (meaning CH_4, C_2H_2, C_2H_4 and other stable species for catalytic dissociation) on the particle surface is rate limiting, an increase will result in an increase in growth rate [39]. Very high hydrocarbon fractions adversely affect growth rate because of excessive amorphous carbon production.

6. Growth mechanisms

Nanotube growth on catalyst particles is similar to a traditional gas–solid interaction process such as thin film deposition on substrates. The growth proceeds according to the following sequence of steps and one or more of these steps may be rate controlling, which varies from case to case and requires careful experimental analysis:

(i) Diffusion of precursor(s) through a thin boundary layer to the substrate.
(ii) Adsorption of species onto the surface.
(iii) Surface reactions leading to film growth.
(iv) Desorption of product species.
(v) Diffusion of species through the boundary layer into the bulk stream.

In low temperature plasmas, the positive ion bombardment of the surface may provide the energy needed in step (iii) or aid in the desorption in step (iv).

In common processes in IC manufacturing such as deposition of silicon, aluminium, silicon nitride, etc, extensive studies have been performed to identify rate controlling steps and understand surface processes. The diamond literature also features numerous such studies. Unfortunately in CNT growth, there have been no careful experimental investigations yet on this subject. However, earlier studies on carbon filaments in the 1970s discuss the process sequence described above [45, 46]. A hydrocarbon such as methane adsorbed onto the catalytic particle surface releases carbon upon decomposition which dissolves and diffuses into the particle. When a supersaturated state is reached, carbon precipitates in a crystalline tubular form. At this juncture two different scenarios are possible. If the particle adherence to the surface is strong, then carbon precipitates from the top surface of the particle and the filament continues to grow with the particle anchored to the substrate. This is called the base growth model. In cases where the particle attachment to the surface is weak, then carbon precipitation occurs at the bottom surface of the particle and the filament lifts the particle as it grows. In this case, the top end of the filament is decorated with the catalyst particle, and this scenario is aptly called the tip growth model. Baker and coworkers [45,46] arrived at the above mechanisms for carbon filament growth based on temperature dependent growth rates, activation energy for various steps, and electron microscopy observations. It is commonly believed in the CNT community now that the mechanisms for the filament growth apply, by extension, to the growth of their nanoscale cousins as well [9,54]. The major reason is the visual observation of catalyst particles on the top or bottom ends as was the case with filament studies.

Prior to understanding surface kinetics, it is important to catalogue the species that arrive at the catalyst particle surface. It is almost unambiguous that in thermal CVD, the (undiluted) hydrocarbon feedstock dissociates catalytically at

the particle surface. Care is taken to maintain the temperature below that for gas phase pyrolysis. As mentioned before, mass spectroscopy studies [49] and modelling [43] confirm this, though amorphous carbon deposits on and around CNTs have been seen due to minimal pyrolysis at the growth temperature.

In the case of PECVD, extensive dissociation in the plasma is expected. A zero-dimensional analysis of a high density plasma shows that a methane/H_2 mixture is thoroughly dissociated (see figures 10–12). The analysis considers electron impact, charge exchange, and neutral reactions but no surface reactions as these are very much unknown. Mass balance equations for neutrals, ions and electrons, and electron and gas energy balance equations are solved; details can be found in [37, 43]. Figures 10–12 show mole fraction of various neutral species as functions of pressure, absorbed power, and methane/hydrogen ratio. First it is interesting to note that at 3 Torr, nearly 95% of the incoming methane is dissociated. Methane dissociation proceeds not only due to electron impact but also due to hydrogen abstraction reaction ($CH_4 + H \rightarrow CH_3 + H_2$). Atomic hydrogen is generated from electron impact of H_2. The largest constituent of the plasma is H_2 since various reactions generate H and H_2, and atomic

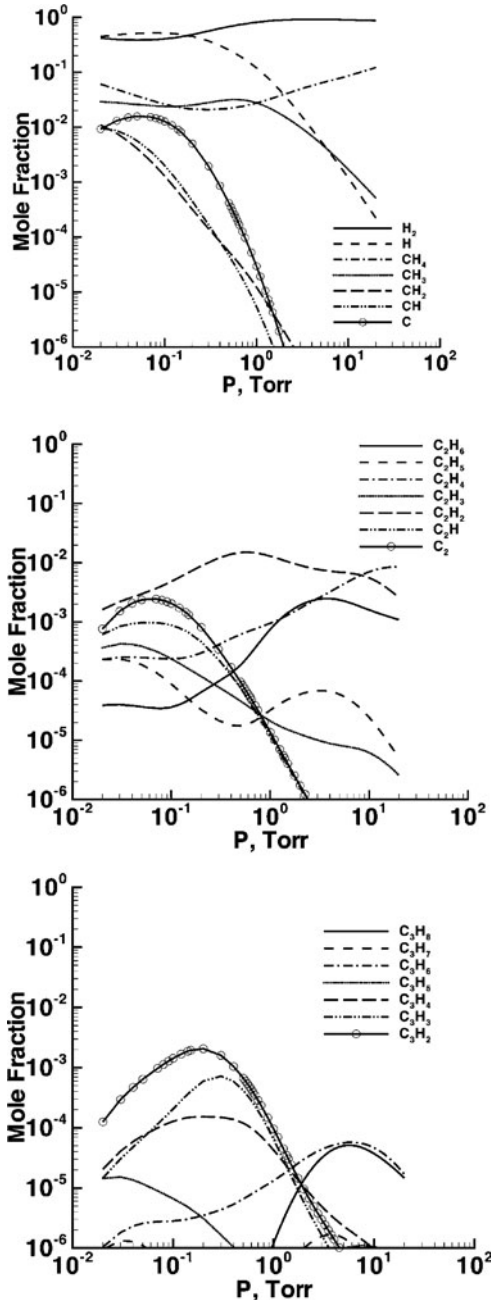

Figure 10. Effect of pressure on neutral composition computed using a zero-dimensional model. Absorbed power = 100 W, total flow rate of 100 sccm with $CH_4 : H_2 = 20 : 80$˚C, and 900˚C.

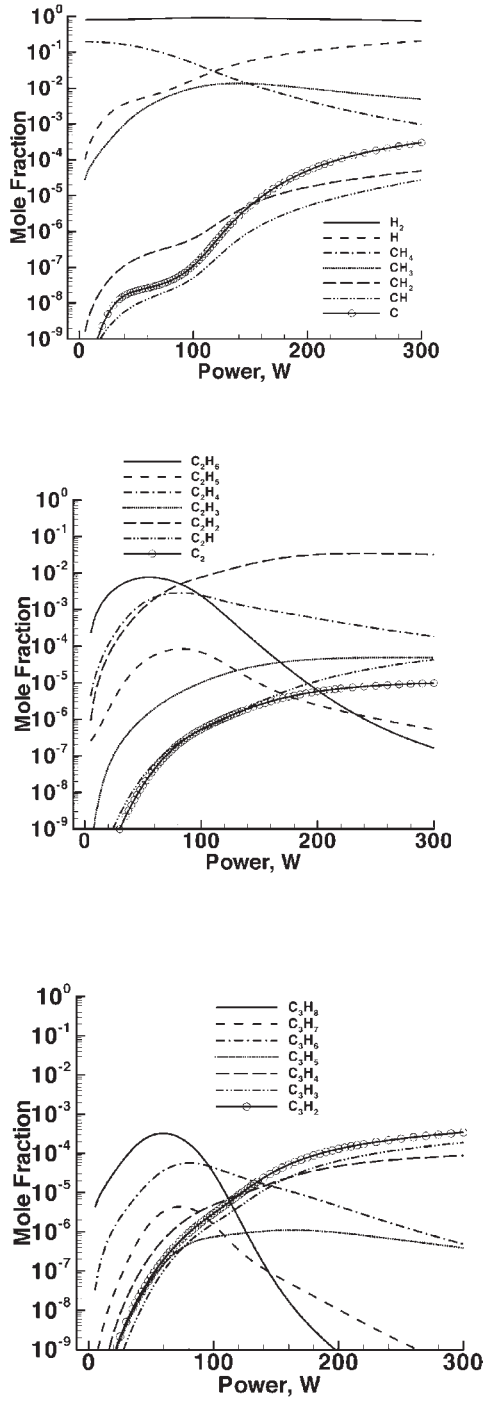

Figure 11. Effect of absorbed power on neutral composition computed using a zero-dimensional model at 3 Torr; other conditions are as in figure 10.

hydrogen recombination also regenerates H_2 at high pressures as evident from figure 10.

In addition to various CH_x, C_2H_y, and C_3H_z radicals, a number of stable species such as C_2H_2, C_2H_4, and C_3H_8 are generated. Note that these stable hydrocarbons dissociate at lower temperatures on transition metal than methane. Kanzow and Ding [55] suggest that SWCNT growth requires (i) temperatures of 900˚C in order to have enough kinetic energy in the system for the layer to bend and form a small cap and (ii) also a low carbon supply on the particle surface. This is why SWCNT growth using thermal CVD is mainly from CO or CH_4 feedstock and at temperatures of 900–1000˚C [7–10]; any exceptions tend to have MWCNTs mixed in the product. Plentiful production of higher hydrocarbons in PECVD would make it difficult to produce SWCNTs; indeed, the lowest number of walls seen to date using PECVD is two [37]. The active radicals, in reasonable abundance in the plasma, may lead to amorphous carbon deposits. It is also likely that atomic hydrogen etches amorphous carbon whereas CNTs are more stable.

The electron density at 3 Torr is $1.4 \times 10^{11}\,cm^{-3}$. By charge balance, the positive ion population is also $1.4 \times 10^{11}\,cm^{-3}$ and it consists of H^+, C^+, CH_y^+, $C_2H_x^+$ ions. It is well known [52] that an increase in power results in an increase in electron density. This would produce increased amounts of H through electron impact dissociation of H_2. An increase in electron density and atomic hydrogen would lead to greater dissociation of methane (figure 11) as power increases, due to electron impact and hydrogen abstraction. Production of acetylene increases steadily with power until it levels off around 300 W, at 3 Torr and 80˚C. An increase in the fraction of methane in the feedstock also leads to increased production of C_2H_2, C_2H_4, C_3H_8 and most radicals (figure 12).

It was mentioned that CNTs grown by PECVD are more vertically-aligned than CVD-grown structures. The entire height of the growing CNTs is submerged inside the sheath where a large electric field exists in the direction normal to the substrate. Even within PECVD-grown CNTs, the degree of orientation depends on the structure. Whereas MWCNTs grow like towers, MWCNFs can be grown as individual, free-standing structures with more alignment. As mentioned earlier the large bias at the wafer helps to grow these MWCNFs vertically; incidentally, MWCNFs have the particles at the top. When the bias is low or in microwave reactors with no dc substrate bias [17, 20–22, 24, 25], the result has mostly been MWCNTs; these always had particles at the base. Combining these observations on the nature of alignment and location of the particles, Merkulov *et al* [30] proposed an alignment mechanism depicted in figure 13. The electrostatic force F creates a uniform tensile stress across the entire particle/CNT interface, regardless of where the particle is

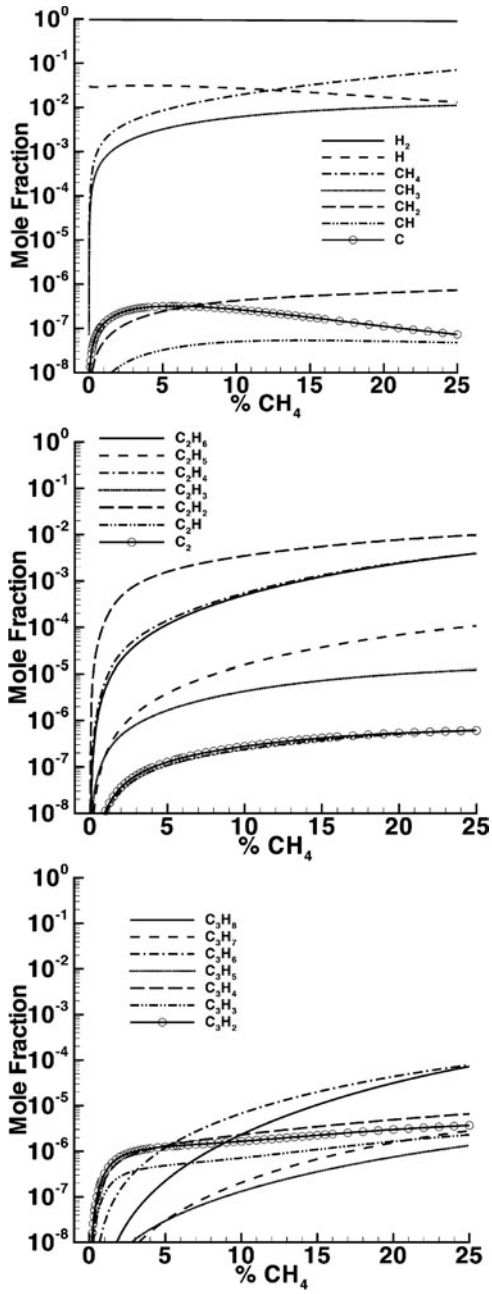

Figure 12. Effect of methane/H_2 ratio at 3 Torr, 100 W absorbed power and 900˚C.

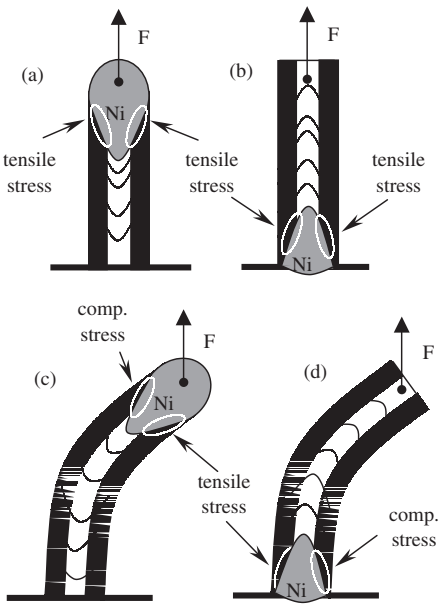

Figure 13. Alignment mechanism as proposed by Merkulov *et al* [30]. Reproduced with permission.

located (tip or base). As growth proceeds, CNTs may bend if there are spatial fluctuations in the carbon precipitation; this would lead to nonuniform stresses at the particle/CNT interface. When the particle is at the top, the electrostalic force F produces a compressive force at the CNT/particle interface where a greater growth rate is seen (figure 13(*c*)); on the side where less growth rate happens, a tensile stress is applied at the interface. This opposite behaviour favours subsequent carbon precipitation at the interface with tensile stress (and a smaller rate of growth). The net result is a stable, negative feedback that works to equalize the growth rate everywhere, and vertical orientation is maintained. When the catalyst particle is at the base, the stress at the interface with the higher growth rate is tensile; this acts to further increase the rate at the same location, causing further bending of the structure. This is essentially an unstable positive feedback system. Though the above argument by Merkulov *et al* appears to be plausible, further work is needed to explain many of the observations. For example, why the tip-grown vertical CNTs happen to be MWCNFs and the base-grown structures are MWCNTs needs to be explained.

7. CNT applications

SWCNTs have been investigated for diodes and transistors, although CNT-based nanoelectronics is really a long-term prospect. Most early transistor demonstrations [56, 57] used SWCNTs from laser ablation samples transplanted to the gap between the source and drain contacts. It would be ideal if the SWCNT could be grown *in situ*, although growth of a nanotube across two contacts horizontally is against the natural growth direction, which is vertical. SWCNTs and MWCNTs can be used as interconnects in silicon IC manufacturing as their current carrying capacity exceeds 10^7 A cm^{-2}. Also, the very high thermal conductivity of the CNTs has potential for their use in dissipating heat from the chips. SWCNTs, when they become available in large quantities, would be useful to develop high strength, low weight composites for a variety of structural applications. Bulk nanotubes are also being investigated for applications in gas absorption, gas separation, and as catalyst support. Gas (such as H_2) or metal (such as Li) storage in nanotubes is an active area of research for energy applications. A discussion of these applications can be found in [4].

A SWCNT or MWCNT grown directly on an AFM cantilever has been shown to be a robust, high-resolution tip for atomic scale imaging [58, 59]. Whereas conventional silicon probes either wear out quickly or even break, CNT tips wear only slowly. Imaging of metallic, semiconductor and dielectric surfaces [59], DNAs [38] and proteins with atomic scale resolution has been demonstrated. The use of MWCNT tips for profilometry [60] in IC manufacturing has also been demonstrated where the need exists to map the depth and shape of holes and trenches. These demonstrations have led to the active development of scaleup techniques to produce hundreds of CNT tip cantilevers on a wafer compared to the current one-at-a-time production. PECVD would be an ideal technique to accomplish this, both in terms of scaleup and probe orientation, as long as one can maintain material quality.

The ability to grow MWCNTs and MWCNFs on patterned substrates has potential applications in field emitters which are being considered for flat panel displays for TV and computer screens and large outdoor displays (see [4]). Verically aligned MWCNFs, which are free-standing, appear to be suitable as electrodes. An array of such MWCNFs reinforced with SiO_2 (in the space between individual tubes) for isolation and mechanical stability has been demonstrated [61]; such gap-filled arrays can be used in biosensor development where DNA is attached to individual fibre ends [62]. This type of array has also been considered for the development of infrared detectors [63]. The general approach of producing gap-filled MWCNF arrays has been advocated as a process solution to CNT interconnects [64]. For a more detailed discussion on applications, the reader is referred to [3, 4].

8. Challenges and future directions

PECVD-grown CNT structures have much application potential as described above. Application development, as expected, is receiving much attention. Successful applications and large scale production processes depend on understanding of several important issues which are listed below.

- What are the species that are responsible for nanotube growth?
- What is the role of atomic hydrogen?
- Are the radicals deleterious? Do they lead to amorphous carbon contamination?
- Is amorphous carbon preferentially etched away compared to nanotubes?
- Is there a specific role for ions related to growth?
  Do they weaken the particle adhesion to the surface?
  If so, what is the dependence on ion energy?
- Is there a preferred hydrogen-carrying diluent (H_2 versus NH_3)?
- What is the role of other diluents such as argon or nitrogen?
- Catalyst effects in terms of the transition metal choice, method of depositing the catalyst, layer thickness, pretreatment if any, particle creation, effect of particle size on nanotube diameter and growth rate.
- Is it possible to grow SWCNTs by PECVD? How?
- Can disorders be annealed away?
- PECVD-grown MWCNTs versus MWCNFs: parameters dictating this choice.
- Rate determining step(s) in CNT growth.
- Tip versus base growth: effect of process parameters
- Alignment mechanism
- How does electric field influence growth orientation and resulting alignment?
- Is there a preferred substrate heating method (resistive heating, hot-filament, IR lamp . . .)?
- How low a growth temperature is possible? This is critical for large area flat panels on glass substrates.
- Is a large dc bias appropriate? Does it damage the CNT structure? What is the effect of the substrate bias on growth rate, structure, and alignment?
- Why is the sub-100 mTorr operation common in IC manufacturing not that common in PECVD of CNTs? What is the effect of pressure? What is the effect of other process parameters?

- Is it possible to obtain growth uniformities over large areas common in IC manufacturing?

Understanding of the issues listed above is important for further progress in this field. Careful diagnostics and modelling studies can help, as successfully demonstrated by the low temperature plasma processing community in IC manufacturing. While the CNT literature is full of recipes, growth results and application potential, diagnostics and modelling are almost nonexistent. It is hoped that the enormous potential of CNTs would stimulate interest in such complementary studies.

Acknowledgment

Work by Alan Cassell was funded by a NASA contract to Eloret Corporation.

References

[1] Iijima S 1991 *Nature* **354** 56
[2] Saito R, Dresselhaus G and Dresselhaus M S 1998 *Physical Properties of Carbon Nanotubes* (London: Imperial College Press)
[3] Meyyappan M and Srivastava D 2003 *Carbon Nanotubes: Handbook of Nanoscience, Engineering, and Technology* (Boca Raton, FL: CRC Press)
[4] Dresselhaus M S, Dresselhaus G and Avouris Ph (ed) 2001 *Carbon Nanotubes* (Berlin: Springer)
[5] Guo T, Nikolev P, Thess A, Colbert D T and Smalley R E 1995 *Chem. Phys. Lett.* **243** 49
[6] Kiang C H, Goddard W A, Beyers R and Bethune D 1995 *Carbon* **33** 903
[7] Dai H, Rinzler A G, Nikolaev P, Thess A, Colbert D T and Smalley R E 1996 *Chem. Phys. Lett.* **260** 471
[8] Hafner J H, Bronikowski M J, Azamian B R, Nikolaev P, Rinzler A G, Colbert D T, Smith K A and Smalley R E 1998 *Chem. Phys. Lett.* **296** 195
[9] Kong J, Soh H T, Cassell A M, Quate C F and Dai H 1998 *Nature* **395** 878
[10] Delzeit L, Chen B, Cassell A M, Stevens R, Nguyen C and Meyyappan M 2001 *Chem. Phys. Lett.* **348** 368
[11] Delzeit L, Nguyen C V, Chen B, Stevens R, Cassell A, Han J and Meyyappan M 2002 *J. Phys. Chem.* B **106** 5629
[12] Cassell A M, Verma S, Delzeit L and Meyyappan M 2001 *Langmuir* **17** 266
[13] Chen B, Parker III G, Han J, Meyyappan M and Cassell A 2002 *Chem. Mater.* **14** 1891
[14] Li J, Papadopoulos C, Xu J M and Moskovits M 1999 *Appl. Phys. Lett.* **75** 367
[15] Chen Y, Wang Z L, Yin J S, Johnson D J and Prince R H 1997 *Chem. Phys. Lett.* **272** 178
[16] Chen Y, Guo L P, Johnson D J and Prince R H 1998 *J. Cryst. Growth* **193** 342
[17] Qin L C, Zhou D, Krauss A R and Gruen D M 1998 *Appl. Phys. Lett.* **72** 3437
[18] Ren Z F, Huang Z P, Xu J W, Wang J H, Bush P, Siegel M P and Provencio P N 1998 *Science* **282** 1105
[19] Tsai S H, Chao C W, Lee C L and Shih H C 1999 *Appl. Phys. Lett.* **74** 3462
[20] Zhang Q, Yoon S F, Ahn J, Gan B, Rusli and Yu M B 2000 *J. Phys. Chem. Solids* **61** 1179
[21] Choi Y C, Lee Y H, Lee B S, Park G, Choi W B, N Lee S and Kim J M 2000 *J. Vac. Sci. Technol.* A **18** 1864
[22] Choi Y C, Shin Y M, Lim S C, Bae D J, Lee Y H, Lee B S and Chung D 2000 *J. Appl. Phys.* **88** 4898
[23] Okai M, Muneyoshi T, Yaguchi T and Sasaki S 2000 *Appl. Phys. Lett.* **77** 3465
[24] Bower C, Zhu W, Jin S and Zhou O 2000 *Appl. Phys. Lett.* **77** 830
[25] Bower C, Zhou O, Zhu W, Werder D J and Jin S 2000 *Appl. Phys. Lett.* **77** 2767
[26] Cui H, Zhou O and Stoner B R 2000 *J. Appl. Phys.* **88** 6072
[27] Merkulov V I, Lowndes D H, Wei Y Y, Eres G and Voelkl E 2000 *Appl. Phys. Lett.* **76** 3555
[28] Wei Y Y, Eres G, Merkulov V I and Lowndes D H 2001 *Appl. Phys. Lett.* **78** 1394
[29] Merkulov V I, Guillorn M A, Lowndes D H, Simpson M L and Voelkl E 2001 *Appl. Phys. Lett.* **79** 1178
[30] Merkulov V I, Melechko A V, Guillorn M A, Lowndes D H and Simpson M L 2001 *Appl. Phys. Lett.* **79** 2970
[31] Ho G W, Wee A T S, Lin J and Tjiu W C 2001 *Thin Solid Films* **388** 73
[32] Teo K B K, Chhowalla M, Amaratunga G A J, Milne W I, Hasko D G, Pirio G, Legagneux P, Wyczisk F and Pribat D 2001 *Appl. Phys. Lett.* **79** 1534
[33] Chhowalla M, Teo K B K, Ducati C, Rupersinghe N L, Amaratunga G A J, Ferrari A C, Roy D, Robertson J and Milne W I 2001 *J. Appl. Phys.* **90** 5308
[34] Teo K B K, Chhowalla M, Amaratunga G A J, Milne W I, Pirio G, Legagneux P, Wyczisk F, Olivier J and Pribat D 2002 *J. Vac. Sci. Technol.* B **20** 116
[35] Tanemura M, Iwata K, Takahashi K, Fujimoto Y, Okuyama F, Sugie H and Filip V 2001 *J. Appl. Phys.* **90** 1529
[36] Tsai C L, Chen C F and Wu L K 2002 *Appl. Phys. Lett.* **81** 721
[37] Delzeit L, McAninch I, Cruden B A, Hash D, Chen B, Han J and Meyyappan M 2002 *J. Appl. Phys.* **91** 6027
[38] Delzeit L, Nguyen C V, Stevens R M, Han J and Meyyappan M 2002 *Nanotechnology* **13** 280
[39] Matthews K, Cruden B, Chen B, Meyyappan M and Delzeit L 2001 *J. Nanosci. Nanotechnol.* **2** 475
[40] Kuttel O M, Groening O, Emmenbegger C and Schlapbach L 1998 *Appl. Phys. Lett.* **73** 2113
[41] Han J, Yang W S, Yoo J B and Park C Y 2000 *J. Appl. Phys.* **88** 7363
[42] Han J *et al* 2002 *J. Appl. Phys.* **91** 483
[43] Hash D and Meyyappan M 2003 *J Appl. Phys.* **93** 750
[44] Nolan D, Lynch D C and Cutler A H 1998 *J. Phys. Chem.* B **102** 4165
[45] Baker R T K, Barber M A, Harris P S, Feates F S and Waite R J 1972 *J. Catal.* **26** 51
[46] Baker R T K, Harris P S, Thomas R B and Waite R J 1973 *J. Catal.* **30** 86
[47] Tibbetts G G 1983 *Appl. Phys. Lett.* **42** 666
[48] Tibbetts G G 1984 *J. Cryst. Growth* **66** 632
[49] Franklin N R and Dai H 2002 *Adv. Mater.* **12** 890
[50] Satake N, Jeong G H, Hirata T, Hatakeyama R, Ishida H, Tohji K and Motomiya K 2002 *Physica* B **323** 290
[51] Ishida H, Satake N, Jeong G H, Abe Y, Hirata T, Hatakeyama R, Tohji K and Motomiga K 2002 *Thin Solid Films* **407** 26
[52] Lieberman M A and Lichtenberg A J 1994 *Principles of Plasma Discharges and Materials Processing* (New York: Wiley)
Popov O A (ed) 1995 *High Density Plasma Sources* (Noyes Publications)
[53] Kortshagen U, Gibson N D and Lawler J E 1996 *J. Phys. D: Appl. Phys.* **29** 1224
[54] Sinnott S B, Andrews R, Qian D, Rao A M, Mao Z, Dickey E C and Derbyshire F 1999 *Chem. Phys. Lett.* **315** 25
[55] Kanzow H and Ding A 1999 *Phys. Rev.* B **60** 11180
[56] Martel R, Schmidt T, Shea H R and Avouris Ph 1998 *Appl. Phys. Lett.* **73** 2447
[57] Tans S J, Verschueren A R M and Dekker C 1998 *Nature* **393** 49

[58] Hafner J H, Cheung C L and Lieber C M 1999 *J. Am. Chem. Soc.* **121** 9750
[59] Nguyen C V, Chao K-J, Stevens R, Delzeit L, Cassell A M, Han J and Meyyappan M 2001 *Nanotechnology* **12** 363
[60] Nguyen C V, Stevens R, Barber J, Han J and Meyyappan M 2002 *Appl. Phys. Lett.* **81** 901
[61] Li J, Stevens R, Delzeit L, Ng H T, Cassell A, Han J and Meyyappan M 2002 *Appl. Phys. Lett.* **81** 910
[62] Nguyen C V, Delzeit L, Cassell A M, Li J, Han J and Meyyappan M 2002 *NanoLett.* **2** 1079
[63] Xu J M 2001 *Infrared Phys. Tech.* **42** 455
[64] Li J, Ye Q, Cassell A, Ng H T, Stevens R, Han J and Meyyappan M 2003 *Appl. Phys. Lett.* **82**